Journal of Biomolecular NMR, 9 (1997) 359–369

J-Bio NMR 437

Temperature dependence of ^{1}H chemical shifts in proteins

Nicola J. Baxter and Michael P. Williamson*

Krebs Institute, Department of Molecular Biology and Biotechnology, University of Sheffield, Firth Court, Western Bank, Sheffield S10 2TN, U.K.

Received 20 November 1996
Accepted 14 February 1997

Keywords: ^{1}H NMR; Chemical shift temperature coefficients; Amide exchange; Hydrogen bonds

Summary

Temperature coefficients have been measured by 2D NMR methods for the amide and $C^{\alpha}H$ proton chemical shifts in two globular proteins, bovine pancreatic trypsin inhibitor and hen egg-white lysozyme. The temperature-dependent changes in chemical shift are generally linear up to about 15° below the global denaturation temperature, and the derived coefficients span a range of roughly –16 to +2 ppb/K for amide protons and –4 to +3 ppb/K for $C^{\alpha}H$. The temperature coefficients can be rationalized by the assumption that heating causes increases in thermal motion in the protein. Precise calculations of temperature coefficients derived from protein coordinates are not possible, since chemical shifts are sensitive to small changes in atomic coordinates. Amide temperature coefficients correlate well with the location of hydrogen bonds as determined by crystallography. It is concluded that a combined use of both temperature coefficients and exchange rates produces a far more reliable indicator of hydrogen bonding than either alone. If an amide proton exchanges slowly and has a temperature coefficient more positive than –4.5 ppb/K, it is hydrogen bonded, while if it exchanges rapidly and has a temperature coefficient more negative than –4.5 ppb/K, it is not hydrogen bonded. The previously observed unreliability of temperature coefficients as measures of hydrogen bonding in peptides may arise from losses of peptide secondary structure on heating.

Introduction

It has been known since the early years of peptide NMR that the chemical shifts of amide proton resonances display a temperature dependence (Ohnishi and Urry, 1969). In general, they shift upfield as the temperature increases and this is conventionally described as a negative temperature coefficient. The rationalization of this effect is that in a hydrogen-bonded amide group, the carbonyl function causes the amide proton to be shifted downfield. On increasing the temperature, the hydrogen bond is weakened (lengthened on average) and the amide proton is shifted downfield to a lesser extent (i.e. a relative upfield shift). The value of the amide proton temperature coefficient has therefore been used widely to predict hydrogen bond donors (Jiménez et al., 1986; Dyson et al., 1988; Andersen et al., 1992; Skalicky et al., 1994), with values more positive than about –5 ppb/K being taken as an indicator that the amide proton is involved in intramolecular hydrogen bonding. However, the theoretical foundation for such a use is flimsy, and there are many examples where the above rule fails: for example, a study of a fairly unstructured peptide in water revealed that most amide protons had 'random-coil'-type temperature coefficients in the range –6 to –10 ppb/K, with one exceptionally large value at –13.5 ppb/K (Williamson et al., 1986). Other experiments demonstrated that this amide proton was in fact involved in a transient hydrogen-bonded structure and thus the large temperature coefficient could be attributed to a loss of secondary structure on heating, rather than reflecting intrinsic hydrogen bonding (see also Andersen et al. (1992)). Similar results observed by a large number of workers have led to the general conclusion that amide temperature coefficients in peptides are poor guides to intramolecular hydrogen bonding.

For these reasons, it has become common, particularly in NMR studies of protein structure, to use amide proton exchange rates instead of temperature coefficients as indi-

*To whom correspondence should be addressed.

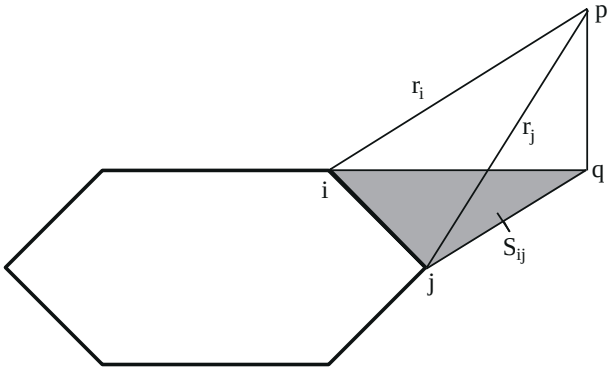

Fig. 1. Geometry for the calculation of ring current shifts using the method of Haigh and Mallion (see text).

cators of hydrogen bonding. Exchange rates are straightforward, although tedious, to measure, and have a sound theoretical basis (Hvidt and Nielsen, 1966; Thomsen and Poulsen, 1993). It might, however, be thought that they are not ideal measures of hydrogen bonding, since they are sensitive to pH (Pedersen et al., 1993), local structure fluctuations (Woodward et al., 1982) and to the presence of a hydrogen-bonded carbonyl group that is in the same peptide bond as the amide proton whose exchange is being measured (Perrin et al., 1990). For peptides in aqueous solution, further practical problems arise, because amide proton exchange rates are often so fast that they are very difficult to determine. In addition, peptides are commonly dissolved in aprotic solvents such as dimethyl sulfoxide, in which amide exchange does not occur. Therefore, the use of these two different measures has tended to become somewhat polarized, with amide temperature coefficients being used to predict hydrogen bond donors in peptides and amide exchange rates being used for the study of hydrogen bonding in proteins.

The purpose of this work is to rationalize the experimentally determined amide proton and $C^{\alpha}H$ temperature coefficients of bovine pancreatic trypsin inhibitor (BPTI) and hen egg-white lysozyme in terms of structural parameters, theoretical chemical shift calculations and amide proton exchange rates.

Theory

Proton chemical shifts in proteins can be calculated adequately by summing terms describing effects from ring current shifts (σ^{ring}), bond magnetic anisotropy (σ^{ani}) and electric field effects (σ^{E}) (Williamson and Asakura, 1993):

$$\sigma^{obs} - \sigma^{random\ coil} = \sigma^{ring} + \sigma^{ani} + \sigma^{E}$$

The least significant of these three terms is the σ^{E} term. For amide protons, the σ^{ani} term tends to dominate, because much of the chemical shift effect on amide protons in proteins comes either from directly bonded hydrogen bond acceptors, particularly carbonyl groups, or from neighboring carbonyl groups (Asakura et al., 1995). For other protons such as $C^{\alpha}H$, ring current shifts can be very significant when the proton is close to aromatic rings; in other cases, the σ^{ani} term is again the most important, and arises principally from the magnetic anisotropy of the peptide bond (Ösapay and Case, 1991; Williamson and Asakura, 1993). The σ^{ani} term is proportional to r^{-3}, where r is the distance between the affected proton and the center of the bond magnetic anisotropy. For a carbonyl bond, this center is close to the oxygen atom which results in large downfield shifts for strongly hydrogen-bonded amide protons (Pardi et al., 1983; Wagner et al., 1983).

As the temperature of a solution is increased, the magnitude of thermal fluctuations becomes larger, which results in an increase in the average distance between atoms. This is evidenced by the reduction in the density of most liquids on heating. In aqueous solutions of peptides and proteins, the chemical shifts of most amide protons move upfield as the temperature is increased. This is normally explained as a weakening of the downfield shift that is the normal consequence of hydrogen bonding, which results from an increase in the average distance between hydrogen bond donor and acceptor. The lengthening of the average hydrogen bond distance will be greater for intermolecular hydrogen bonds (such as bonds to bulk water) than for intramolecular hydrogen bonds, and hence the chemical shift of amide protons hydrogen bonded to water will shift upfield more with temperature than internally hydrogen-bonded amides.

Chemical shift effects are strongly distance dependent, and are therefore governed by very local structural features. We assume that an increase in the temperature of a protein in solution does not produce any gross structural changes (except possibly close to the denaturation temperature), but merely leads to an increase in the local thermal fluctuations. For most protons, one would therefore predict that an increase in temperature would cause chemical shifts to move towards their random-coil positions, as is indeed seen (Andersen, N.H. et al., personal communication). The chemical shift changes expected from such an increase in motion can be modelled either from molecular dynamics simulations or by assuming that the local motions are harmonic. The latter leads to readily calculable formulas for the chemical shift changes expected on heating, since the change in chemical shift will then be given by the second derivative of the shift with respect to the atomic coordinates.

Following the method of Haigh and Mallion (1980), the ring current shift at a point p can be calculated as

$$\sigma = kB \sum_{pairs} \left(r_i^{-3} + r_j^{-3} \right) S_{ij}$$

where k is a ring current intensity factor, which accounts for differences in the electronic structure of the ring from

that of benzene, B is a constant of proportionality related to the susceptibility of the ring, S_{ij} is the area formed by ring atoms i and j and point q (the projection of p into the plane of the ring), and the summation runs over all adjacent pairs of ring atoms (Fig. 1).

S_{ij} can be calculated as

$$S_{ij} = \frac{1}{2}\left(\mathbf{r}_i \cdot \mathbf{r}_j \wedge \mathbf{r}_n\right)$$

where the bold characters denote vectors, and $\mathbf{r}_n$ is the vector pq. The partial derivative of the area with respect to an orthogonal coordinate direction vector **x** is

$$\frac{\partial S_{ij}}{\partial x} = -\frac{1}{2}\left(\mathbf{r}_j - \mathbf{r}_i\right) \wedge \mathbf{r}_{nx}$$

where $\mathbf{r}_{nx}$ is the component of $\mathbf{r}_n$ in the x direction. By application of the chain rule for differentiation,

$$\frac{\partial \sigma}{\partial x} = -\frac{kB}{2}\sum_{pairs}\left[\left(r_i^{-3} + r_j^{-3}\right)\left\{\left(\mathbf{r}_j - \mathbf{r}_i\right) \wedge \mathbf{r}_{nx}\right\} + 3\left(\mathbf{r}_i \cdot \mathbf{r}_j \wedge \mathbf{r}_n\right)\left\{\left(x_i - x_p\right)r_i^{-5} + \left(x_j - x_p\right)r_j^{-5}\right\}\right]$$

and similarly

$$\frac{\partial^2 \sigma}{\partial x^2} = -\frac{3kB}{2}\sum_{pairs}\left\{S_{ij}\left[5\left(x_i - x_p\right)^2 r_i^{-7} + 5\left(x_j - x_p\right)^2 r_j^{-7} + r_i^{-5} + r_j^{-5}\right] + 2\left(\mathbf{r}_j - \mathbf{r}_i\right) \wedge \mathbf{r}_{nx}\left[\left(x_i - x_p\right)r_i^{-5} + \left(x_j - x_p\right)r_j^{-5}\right]\right\}$$

For the overall temperature dependence of the ring current shift, the quantity $\nabla^2\sigma$ was calculated.

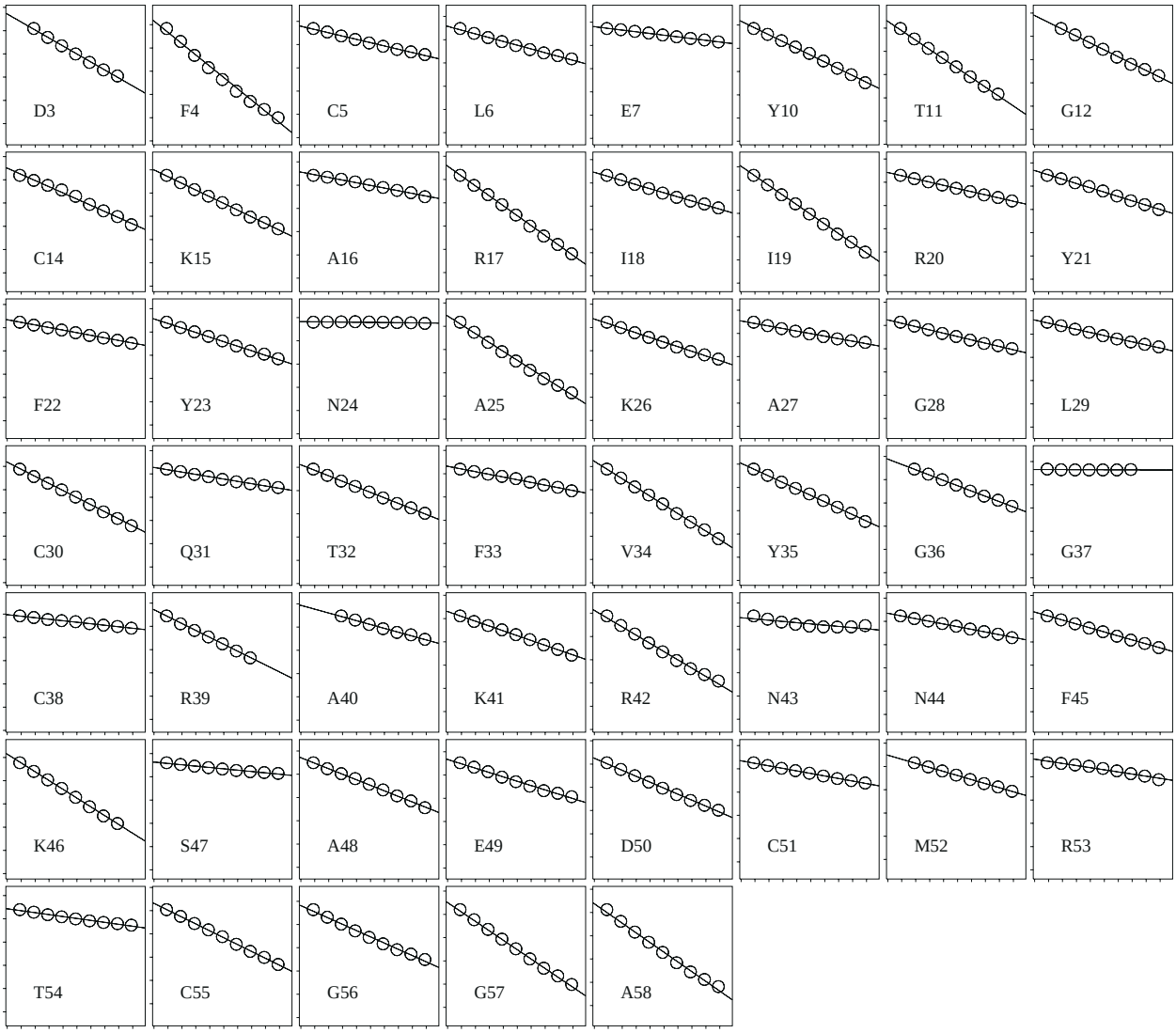

Fig. 2. Dependence of chemical shift on temperature for the backbone amide protons of BPTI at pH 4.6. The best-fit lines are indicated. The x-axis for each graph displays the range 269–369 K with tick marks at 10° intervals. The scaling on the y-axis is identical for each plot; the tick mark interval corresponds to 0.2 ppm.

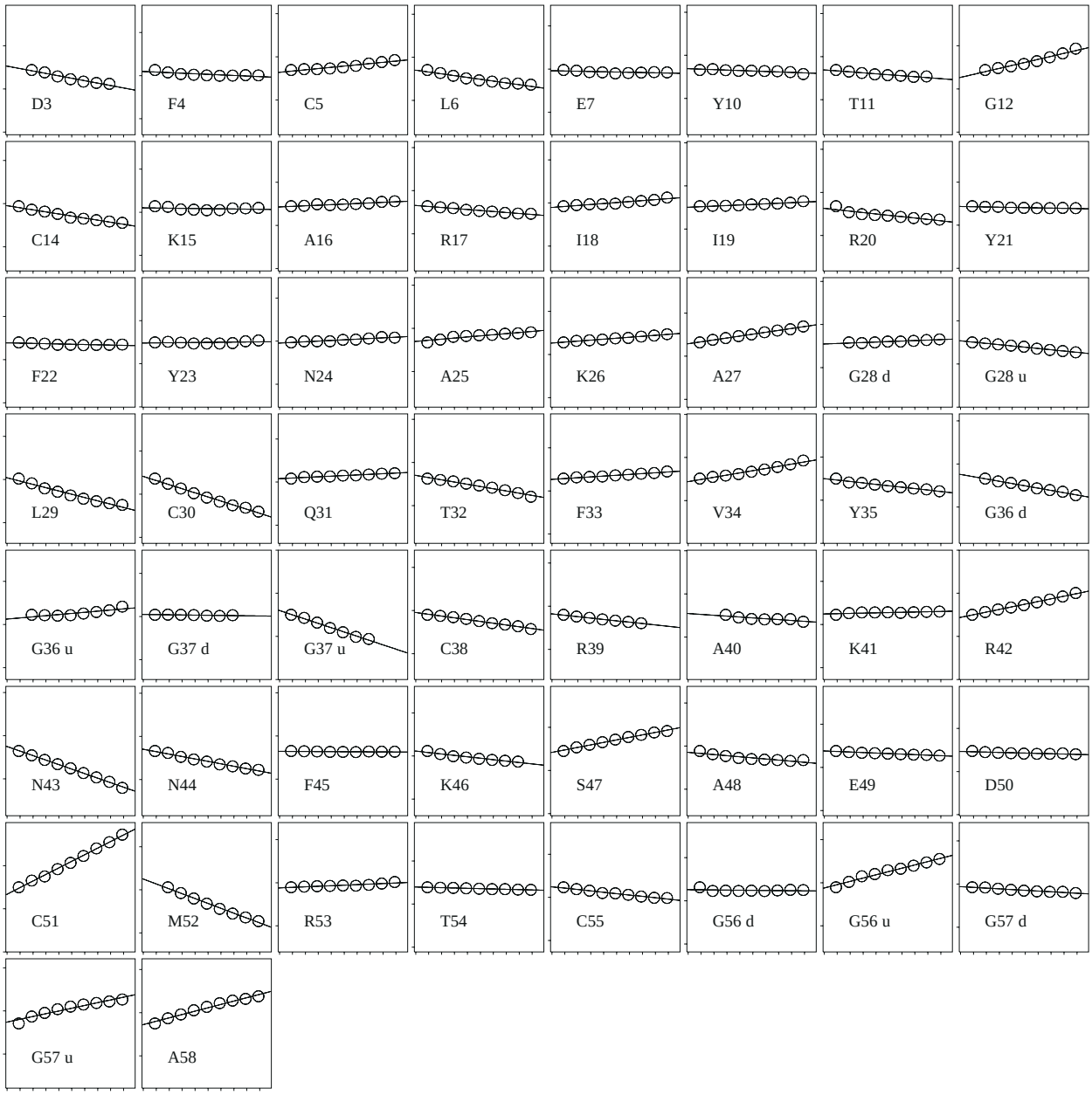

Fig. 3. Plots of $C^{\alpha}H$ chemical shift against temperature and their best-fit lines for BPTI at pH 4.6. The x-axis for each graph displays the range 269–369 K with tick marks at 10° intervals. The scaling on the y-axis is identical for each plot; the tick mark interval corresponds to 0.2 ppm. For the glycine residues, d and u correspond to the downfield and upfield $C^{\alpha}H$ resonances, respectively.

Materials and Methods

Sample preparation

Bovine pancreatic trypsin inhibitor and hen egg-white lysozyme were obtained from Sigma and were used without further purification. Samples of BPTI (4.6 mM, 0.5 ml) adjusted to pH 3.4 and pH 4.6, and samples of lysozyme (7.0 mM, 0.5 ml) adjusted to pH 3.8 and pH 5.0 were prepared in 90% H_2O/10% D_2O. Internal 3-trimethylsilyl-2,2,3,3,-d_4-propionate sodium salt (TSP) served as the reference for ^1H chemical shifts. No correction was made for the temperature dependence of TSP or for any temperature-dependent pH changes.

NMR spectroscopy

All NMR spectra were acquired using a Bruker AMX-500 spectrometer and were processed and displayed using FELIX (Biosym Technologies Inc., San Diego, CA, U.S.A.) operating on a Silicon Graphics workstation. For the determination of the NH and $C^{\alpha}H$ temperature coefficients, TOCSY spectra were recorded at 10° intervals from 279 K to 359 K for BPTI and from 278 K to 328 K

for lysozyme. NOESY experiments were acquired for the purposes of ^{1}H chemical shift assignment at 309 K for BPTI and 308 K for lysozyme. The probe temperature was calibrated by measuring the peak separation in ppm between the OH and CH_2 resonances of ethylene glycol and using a temperature calibration curve provided by Bruker. The TOCSY and NOESY experiments were recorded with water presaturation in phase-sensitive mode using TPPI typically into 500, 4K complex files, with 64 scans per increment and spectral widths of 12.5 kHz in F2 and 6.25 kHz in F1. The TOCSY spin-lock was achieved by a 100 ms DIPSI-2 pulse sequence at a field strength of 10.9 kHz and the NOESY mixing time was 150 ms for BPTI and 200 ms for lysozyme. A Hahn echo delay of 2.54 ms was inserted in the pulse sequences prior to data acquisition for the application of a time-domain Gaussian convolution filter (over 32 points) to remove the solvent signal (Waltho and Cavanagh, 1993). The TOCSY and NOESY t_2 data were left-shifted by 32 complex points and sine-squared bell apodization functions shifted by 60° were applied in both dimensions. The data were Fourier transformed into $4K \times 2K$ ($F2 \times F1$) real points and the spectral widths and the number of points in F2 were halved during processing, by the removal of 1K real points from both edges of the spectrum, resulting in a $2K \times 2K$ real matrix with spectral widths of 6.25 kHz in both F1 and F2.

Determination of temperature coefficients

Sequential TOCSY spectra of the temperature series were overlaid within FELIX and the NH-C$^\alpha$H cross peaks were assigned by using the database facility. The fitting program, written in FORTRAN, performed a least-squares minimization of a linear equation to the chemical shift versus temperature data, and the NH and C$^\alpha$H temperature coefficients were obtained from the gradient of the best-fit line. Graphical display of the fitted and experimental data was achieved using the POSTSCRIPT programming language (Adobe Systems Inc., Mountain View, CA, U.S.A.) on a Silicon Graphics workstation. Correlation analysis and χ^2 tests were performed in EXCEL 5.0 (Microsoft Corporation, Redmond, WA, U.S.A.). For the χ^2 test, the numerical data were rank ordered and divided into three equal bins. The significance values are those appropriate for two degrees of freedom (except for the comparison of exposure with hydrogen bonding, which has only one degree of freedom).

TABLE 1
AMIDE PROTON AND C$^\alpha$H CHEMICAL SHIFT TEMPERATURE DEPENDENCES FOR BPTI AT pH 3.4 AND pH 4.6

Residue	NH Δδ/ΔT (ppb/K)		C$^\alpha$H Δδ/ΔT (ppb/K)		Residue	NH Δδ/ΔT (ppb/K)		C$^\alpha$H Δδ/ΔT (ppb/K)	
	pH 3.4	pH 4.6	pH 3.4	pH 4.6		pH 3.4	pH 4.6	pH 3.4	pH 4.6
D3	–7.49	–6.88	–1.18	–1.12	F33	–2.43	–2.32	0.38	0.38
F4	–10.92	–9.70	–1.11	–0.26	V34	–7.83	–7.50	0.95	1.02
C5	–2.79	–2.83	0.70	0.58	Y35	–5.75	–5.53	–0.80	–0.66
L6	–3.53	–3.25	–0.89	–0.84	G36	–5.04	–4.57	–1.11, 0.57	–1.06, 0.52
E7	–0.93	–1.46	–0.73	–0.12	G37	–0.09	–0.05	–0.22, –1.23	–0.08, –1.99
Y10	–6.30	–5.84	–0.40	–0.21	C38	–1.37	–1.30	–0.88	–0.83
T11	–8.39	–8.08	–0.49	–0.45	R39	–6.25	–5.95	–0.53	–0.64
G12	–6.20	–5.91	1.30	1.39	A40	–3.54	–3.31	–0.15	–0.40
C14	–5.65	–5.33	–0.91	–0.96	K41	–3.96	–4.15	–0.31	0.13
K15	–5.86	–5.76	0.03	–0.07	R42	–7.16	–7.09	1.00	1.23
A16	–2.29	–2.29	0.37	0.27	N43	–2.23	–1.07	–2.19	–2.09
R17	–8.85	–8.53	–0.34	–0.47	N44	–2.49	–2.30	–1.09	–1.13
I18	–3.63	–3.52	0.46	0.45	F45	–3.53	–3.42	–0.17	–0.03
I19	–8.61	–8.28	0.24	0.27	K46	–7.42	–7.56	–0.41	–0.66
R20	–2.85	–2.74	–0.60	–0.64	S47	–1.24	–1.16	1.16	1.16
Y21	–3.89	–3.72	–0.11	–0.11	A48	–4.70	–4.76	–0.63	–0.51
F22	–2.34	–2.23	–0.15	–0.13	E49	–	–3.74	–	–0.24
Y23	–4.45	–3.92	0.12	0.06	D50	–5.32	–5.15	0.01	–0.15
N24	–0.19	–0.13	0.39	0.30	C51	–2.55	–2.17	3.04	3.05
A25	–7.19	–7.63	0.31	0.51	M52	–4.08	–3.50	–2.24	–2.26
K26	–4.24	–3.97	0.54	0.45	R53	–2.65	–1.83	0.22	0.25
A27	–2.29	–2.17	0.92	0.88	T54	–1.49	–1.67	–0.32	–0.15
G28	–2.98	–2.85	0.13, –0.71	0.22, –0.59	C55	–6.21	–5.92	–0.66	–0.64
L29	–2.74	–2.67	–1.53	–1.53	G56	–5.42	–5.37	–0.29, 1.45	–0.06, 1.53
C30	–6.39	–6.09	–1.91	–1.90	G57	–8.43	–8.11	–0.35, 1.15	–0.34, 1.28
Q31	–2.22	–1.99	0.21	0.29	A58	–8.30	–8.35	2.13	1.56
T32	–4.87	–4.74	–1.02	–1.03					

For the C$^\alpha$H temperature coefficients of the glycine residues, the first and second values correspond to the downfield and upfield C$^\alpha$H resonances, respectively.

TABLE 2
AMIDE AND $C^{\alpha}H$ CHEMICAL SHIFT TEMPERATURE DEPENDENCES FOR LYSOZYME AT pH 3.8 AND pH 5.0

Residue	NH Δδ/ΔT (ppb/K)		$C^{\alpha}H$ Δδ/ΔT (ppb/K)		Residue	NH Δδ/ΔT (ppb/K)		$C^{\alpha}H$ Δδ/ΔT (ppb/K)	
	pH 3.8	pH 5.0	pH 3.8	pH 5.0		pH 3.8	pH 5.0	pH 3.8	pH 5.0
V2	–8.92	–8.96	–0.42	–0.16	N59	–7.36	–7.47	–1.19	–0.53
F3	–5.63	–5.26	1.49	1.47	S60	–0.41	0.01	–2.00	–1.75
G4	–3.41	–2.20	–0.33, –1.89	0.24, –1.65	R61	–2.60	–1.82	–0.66	–0.84
R5	–5.66	–4.79	–0.02	0.37	W62	–6.33	–6.41	–0.02	–0.31
C6	–6.49	–6.30	–1.06	–0.82	W63	–0.21	–0.04	–0.41	–0.37
E7	–8.39	–8.44	–0.46	–0.66	C64	–1.26	–0.62	–1.81	–1.54
L8	–5.41	–5.21	–1.38	–1.04	N65	–6.57	–6.54	–3.33	–3.23
A9	–5.57	–5.48	–0.28	–0.21	D66	–14.95	–14.38	–1.26	–1.02
A10	–3.62	–3.54	–1.17	–1.03	G67	–1.49	–0.91	–0.18, –2.66	0.02, –2.15
A11	–1.11	–1.19	–1.97	–2.13	R68	–3.20	–3.00	–2.39	–2.20
M12	–6.76	–7.18	0.41	0.68	T69	–8.05	–7.58	–0.65	–0.61
K13	–2.50	–3.24	–2.17	–1.64	G71	–6.92	–6.19	–0.52, 0.07	–0.46, 0.20
R14	–4.85	–5.69	–0.85	–1.30	S72	–2.48	–2.55	–1.60	–1.83
H15	–2.28	–1.89	–0.18	–0.61	N74	–14.90	–15.12	–1.95	–2.00
G16	–1.45	–1.05	–0.58, 0.88	–0.44, 1.59	L75	–6.47	–6.49	–0.87	–0.72
L17	–1.71	–1.05	0.46	0.87	C76	–5.27	–5.41	–0.50	–0.37
D18	–9.19	–8.95	0.37	0.71	N77	–2.14	–2.12	–0.81	–1.47
N19	–5.73	–5.05	1.35	1.08	I78	–9.12	–8.80	–0.77	–0.70
Y20	–5.43	–5.26	1.58	1.51	C80	–3.35	–2.74	–0.09	0.11
R21	–7.77	–7.20	–1.88	–1.28	S81	–6.38	–6.08	–0.61	–0.33
G22	–3.29	–3.53	–0.34, –0.56	–0.53, –0.20	A82	–2.92	–2.51	–1.11	–0.92
Y23	–2.13	–2.33	–0.37	–0.37	L83	–3.28	–2.90	–1.53	–1.16
S24	–10.83	–10.26	0.78	1.14	L84	–2.09	–1.95	–1.94	–1.53
G26	–6.72	–6.32	–1.40, –0.46	–0.77, –0.26	S85	–2.25	–1.81	–0.11	–0.11
N27	–2.70	–2.44	0.28	–0.16	S86	–9.58	–9.37	–0.66	–0.20
W28	–0.85	–0.52	–0.26	–0.01	D87	–4.29	–3.83	–2.01	–1.75
V29	–3.37	–2.57	–0.72	–0.45	I88	–8.30	–7.78	–3.61	–3.27
C30	–3.58	–1.37	–0.26	–0.29	T89	–5.75	–3.37	–1.13	–1.61
A31	–3.84	–3.87	–0.47	–0.51	A90	–9.03	–9.10	–0.80	–0.46
A32	–2.11	–1.69	–1.21	–1.27	S91	–6.43	–6.34	–1.16	–1.12
K33	–3.41	–2.79	–0.24	–0.14	V92	–5.16	–4.85	0.96	1.01
F34	–2.81	–2.82	–0.77	–0.42	N93	–4.57	–4.66	–0.12	–0.02
E35	–5.08	–4.87	–0.75	–0.59	C94	–1.54	–1.51	–1.65	–1.40
S36	–3.37	–2.97	–1.11	–0.58	A95	–4.75	–4.32	–0.57	–1.01
N37	–0.33	–0.42	–2.68	–2.55	K96	–4.17	–3.49	–0.56	–0.59
F38	–1.12	–0.83	–0.86	–0.63	K97	–0.59	–0.39	–1.15	–0.72
N39	–1.81	–1.49	–1.19	–1.00	I98	–3.64	–	0.83	–
T40	–6.60	–6.18	–0.22	–0.06	V99	–8.13	–7.71	–1.63	–0.97
Q41	–3.55	–3.52	–0.25	–0.26	S100	3.61	2.22	–2.86	–2.57
A42	–2.41	–2.15	–1.10	–1.10	D101	1.54	2.48	1.12	1.05
T43	–8.27	–7.01	–0.61	–0.67	G102	–8.55	–6.79	–4.75, 3.03	0.93, 2.12
N44	–2.57	–1.80	–0.76	–0.10	N103	–4.25	–5.02	–4.09	–4.07
R45	–9.64	–8.87	0.15	0.37	G104	–8.30	–8.31	–1.31, –3.45	–0.77, –3.31
N46	–5.12	–4.23	–0.80	–0.84	M105	–6.58	–7.03	–0.89	1.56
T47	–7.54	–7.05	–0.54	–0.35	N106	–3.02	–2.21	–0.91	–0.45
D48	–4.34	–4.24	–0.42	–0.01	A107	3.15	1.83	–0.12	–0.29
G49	–3.20	–2.89	–1.10, –1.54	–0.99, –1.28	W108	–4.18	–4.01	0.32	–0.08
S50	–4.36	–3.91	–1.71	–1.41	V109	–7.13	–6.87	–0.14	–0.25
T51	–7.16	–6.53	–0.37	–0.47	A110	–2.18	–1.57	–2.54	–1.82
D52	–1.58	–1.91	–0.54	–0.58	W111	–0.01	–0.08	–0.47	–0.25
Y53	–4.46	–4.93	–0.41	–0.06	R112	–6.32	–6.25	0.49	0.39
G54	–	–3.40	–, –	–1.60, 1.40	N113	–5.65	–5.37	0.80	0.61
I55	–9.65	–8.26	–1.30	–0.53	R114	–4.92	–4.55	–1.10	–0.70
L56	–4.71	–4.66	–0.12	0.15	C115	–3.54	–2.89	–1.52	–0.80
Q57	–3.04	–2.46	–0.51	–0.18	G117	–5.13	–4.94	–0.72, –0.53	–0.67, –0.23
I58	–2.35	–2.06	–0.86	–0.50	T118	–3.28	–2.83	–0.71	–0.64

TABLE 2
(continued)

Residue	NH Δδ/ΔT (ppb/K)		$C^{\alpha}H$ Δδ/ΔT (ppb/K)		Residue	NH Δδ/ΔT (ppb/K)		$C^{\alpha}H$ Δδ/ΔT (ppb/K)	
	pH 3.8	pH 5.0	pH 3.8	pH 5.0		pH 3.8	pH 5.0	pH 3.8	pH 5.0
D119	−8.14	−8.01	−1.33	−1.22	R125	−2.42	−1.96	−0.67	−0.56
V120	−5.07	−4.79	−0.50	0.23	G126	−7.20	−6.95	−0.63, −0.83	−0.48, −0.39
Q121	−5.69	−5.16	−1.31	−1.16	C127	−0.97	−0.63	−0.72	−1.04
A122	−2.18	−2.27	−0.65	−0.43	R128	−8.16	−7.91	0.09	0.12
W123	−4.40	−4.40	−0.28	0.08	L129	−8.79	−8.32	−0.73	−0.56
I124	−2.20	−1.87	−1.80	−1.70					

For the $C^{\alpha}H$ temperature coefficients of the glycine residues, the first and second values correspond to the downfield and upfield $C^{\alpha}H$ resonances, respectively.

Calculations

The FORTRAN programs used for the calculation of proton chemical shifts and their second derivatives are available at http://www.shef.ac.uk/~mbb/nmr/home.html. NH and $C^{\alpha}H$ chemical shift calculations were performed on the crystal structures of BPTI (5pti) (Wlodawer et al., 1984) and lysozyme (1lzt) (Kurachi et al., 1976) deposited with the Brookhaven Protein Databank (Bernstein et al., 1977). Solvent-accessible surface areas for the backbone nitrogen atoms were determined using the algorithm of Lee and Richards (1971). Hydrogen bond prediction was performed on 5pti, 1lzt and an additional lysozyme crystal structure 1lse (Kurinov and Harrison, 1995) using several algorithms including those of Kabsch and Sander (1983) and INSIGHT (Biosym Technologies Inc.) in order to obtain a consensus description of hydrogen bond patterns within BPTI and lysozyme. Amide hydrogen exchange rates were taken from Wagner and Wüthrich (1982) (BPTI, p^2H 7.5, 309 K) and Radford et al. (1992) (lysozyme, pH 7.5, 303 K). Crystallographic B factors for BPTI and lysozyme were obtained from their respective Brookhaven Protein Databank coordinate files. For lysozyme, the order parameter (S^2) derived from ^{15}N relaxation data (308 K) was taken from Buck et al. (1995). Experimental proton chemical shifts were converted to secondary shifts by subtraction of the random-coil chemical shifts given by Wüthrich (1986).

Results and Discussion

Assignment of the NH-$C^{\alpha}H$ cross peaks was achieved, following the sequential assignment methodology of Wüthrich and co-workers, by using pairs of TOCSY and NOESY spectra recorded at 309 K for BPTI and 308 K for lysozyme and with reference to published chemical shift data: BPTI (Tüchsen and Woodward, 1987; Wagner et al., 1987) and lysozyme (Redfield and Dobson, 1988; Smith et al., 1993a). The temperature dependences of the NH and $C^{\alpha}H$ chemical shifts for BPTI and lysozyme were determined over a wide temperature range. The experimental and fitted data are presented in Fig. 2 (NH) and Fig. 3 ($C^{\alpha}H$) for BPTI, pH 4.6. The NH and $C^{\alpha}H$ coefficients for BPTI (pH 3.5 and pH 4.6) and lysozyme (pH 3.8 and pH 5.0) are listed in Tables 1 and 2, respectively.

Most proton chemical shifts display a linear temperature dependence, although it is noticeable that many protons show some deviation from linearity at the highest temperature measured. For both proteins, this temperature is about 15° below the melting temperature and, therefore, this behavior may be interpreted as the onset of a global cooperative unfolding event. A few protons exhibit a curved temperature dependence, indicating that at least two species in these regions of the protein are in fast exchange over the temperature range studied. The amide proton chemical shift temperature dependence data for BPTI and lysozyme at the two pH conditions are very similar (Fig. 4: BPTI R = 0.993, lysozyme R = 0.986), implying that there are no major conformational changes between the two pH values, and that protonation of side chains causes only very local changes in chemical shift. This result contrasts with amide exchange rates which display a strong pH dependence (Englander and Kallenbach, 1983; Pedersen et al., 1993).

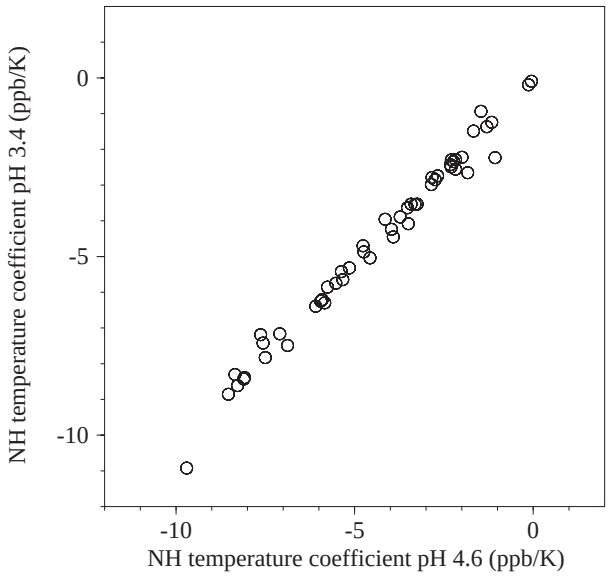

Fig. 4. Comparison of amide proton temperature coefficients for BPTI at pH 4.6 and pH 3.4; R = 0.993.

TABLE 3
CORRELATION OF STRUCTURAL AND NMR PARAMETERS FOR BPTI AND LYSOZYME

	NH $\Delta\delta/\Delta T$	$C^{\alpha}H$ $\Delta\delta/\Delta T$	$\log(R_{ex})$	B factor	S^2	Exposure
BPTI						
$C^{\alpha}H$ $\Delta\delta/\Delta T$	–0.001					
$\log(R_{ex})$	–0.42	0.05				
B factor	–0.36	0.19	0.33			
Exposure	+++	–	+++	–		
H bond	+++	–	+++	–		+++
Lysozyme						
$C^{\alpha}H$ $\Delta\delta/\Delta T$	–0.11					
$\log(R_{ex})$	–0.32	0.05				
B factor	0.01	0.03	0.15			
	–0.16	–0.06	–0.50			
S^2	0.03	0.14	–0.07	–0.06		
Exposure	++	–	+++	–	+++	
	+++	–	+++	++	–	
H bond	+++	–	+++	–	++	+++
	+++	–	+++	–	+++	+++

The values listed are correlation coefficients. NH $\Delta\delta/\Delta T$: temperature coefficient of amide protons (BPTI pH 4.6; lysozyme pH 5.0). $C^{\alpha}H$ $\Delta\delta/\Delta T$: temperature coefficient of $C^{\alpha}H$ (BPTI pH 4.6; lysozyme pH 5.0). R_{ex}: exchange rate of amide protons. The B factor is the crystallographic temperature factor and S^2 is the order parameter determined from ^{15}N relaxation parameters. Surface exposure and presence or absence of hydrogen bonds were assessed on a binary scale (yes or no), and therefore correlation coefficients are not meaningful. The +/– symbols indicate the significance as shown in a χ^2 test: (+++) $p < 0.1$; (++) $1.0 > p > 0.1$; (+) $5.0 > p > 1.0$; (–) $p > 5.0$. For lysozyme, two different crystal structures were used, namely 1lzt (top line) and 1lse (bottom line).

The range of the amide temperature coefficients is 2–3 times that of the $C^{\alpha}H$ temperature coefficients. It is also clear that the mean value of the amide coefficients is negative, while that of the $C^{\alpha}H$ coefficients is close to zero (in BPTI at pH 4.6, $C^{\alpha}H$ -0.1 ± 1.0 ppb/K compared to NH -4.4 ± 2.4 ppb/K). This can be rationalized by the predominantly downfield shift of hydrogen-bonded amide protons, whereas $C^{\alpha}H$ can be shifted almost equally upfield or downfield. As expected from the very local nature of the factors causing structure-dependent chemical shifts, there is no correlation between temperature coefficients for NH and $C^{\alpha}H$ from the same residue ($R = -0.001$).

Correlations

In order to assess the reliability of amide proton temperature coefficients as indicators of hydrogen bond donors, temperature coefficients for BPTI and lysozyme have been correlated with amide proton exchange rates, hydrogen bond patterns and other related parameters, as shown in Table 3. The table shows that there is a reasonable correlation, but certainly not a good correlation, between amide exchange rates and amide proton temperature coefficients. Others have made the same comments (Skalicky et al., 1994; Andersen, N.H., personal communication). The correlations with the consensus presence/absence of hydrogen bond donors are strong for both amide exchange rates and temperature coefficients, although it is worth pointing out that the values of the χ^2 parameter are much higher (i.e. more significant) for temperature coefficients (for BPTI and lysozyme, the χ^2 values for amide exchange rates are 18.1 and 36.4, respectively, while for amide temperature coefficients they are 40.5 and 75.8). It is clear that amide exchange rates also correlate well with exposure: in particular, buried amide protons exchange slowly even if not hydrogen bonded, whereas exposed amides exchange rapidly even if hydrogen bonded (Woodward et al., 1982; Pedersen et al., 1991). Surface exposure is also well correlated to hydrogen bond presence and to amide temperature dependence. It is surprising (but beyond the scope of this study) to note that both the B factor and the order parameter (S^2) correlate poorly with most other parameters.

A more detailed comparison of amide exchange rates and amide proton temperature coefficients for lysozyme is presented in Fig. 5. Similar results were also obtained for BPTI. As anticipated by the remarks above, there are three buried amide protons with slow exchange rates which are not hydrogen bonded to protein acceptors (Ile^{55}, Leu^{56}, Asn^{59}). Conversely, there are a number of strongly hydrogen-bonded amide protons, including many in regular secondary structure, that are exposed and consequently have rapid exchange rates. Thus, the standard assumption that slow exchange rates imply hydrogen bonding is usually true, but by no means always true. By taking all amide protons with temperature coefficients more positive than –4.5 ppb/K as being hydrogen bonded, as indicated by the dashed line in Fig. 5, amide temperature coefficients can be used to predict hydrogen bond donors. This criterion identifies more amide protons than amide exchange studies; in particular, it highlights a large number of exposed protons that are hydrogen bonded and, at least in this example, does not mistakenly include any non-hydrogen-bonded amide protons. Therefore, the two methods are to some extent complementary. It is particularly striking that virtually all of the amide protons displaying fast exchange rates and large negative temperature coefficients are not hydrogen bonded, whereas all of the amides with slow exchange rates and more positive coefficients than –4.5 ppb/K are located in hydrogen-bonded regular secondary structure.

It is of interest to contrast these encouraging results with many of the temperature dependence studies performed on peptides, where it was often found that amide proton temperature coefficients were poor indicators of hydrogen bonding. It is possible that the disappointing results seen with peptides (as opposed to the globular proteins studied here) were due to the occurrence of significant losses of local secondary structure on heating. Therefore, the measured temperature coefficients reflect

the sum of the expected hydrogen bond dependence characterized here and a second term arising from the loss of folded structure with increasing temperature. As shown above, this is not significant in folded proteins until very close to the denaturation temperature. Therefore, we conclude that amide proton temperature coefficients are more reliable measures of hydrogen bonding in globular proteins than they are in peptides.

Calculations of temperature coefficients

It has been shown previously (Williamson et al., 1995) that calculated chemical shifts in proteins depend very strongly on the accuracy of the coordinates. This is particularly true for amide protons, where very small changes in the position of any of the N-H···O=C atoms can cause large changes in the calculated chemical shift (Asakura et al., 1995). Moreover, for amide protons, the chemical shift also depends on the position of any water molecules hydrogen bonded to the amide group, which is often unknown to any useful accuracy. Therefore, it was not expected that there would be any great success in the calculation of the amide temperature coefficients, beyond the obvious generalization that hydrogen-bonded amides have lower (more positive) coefficients than non-hydrogen-bonded amides. Thus, temperature coefficient calculations were restricted to $C^{\alpha}H$, since their chemical shifts

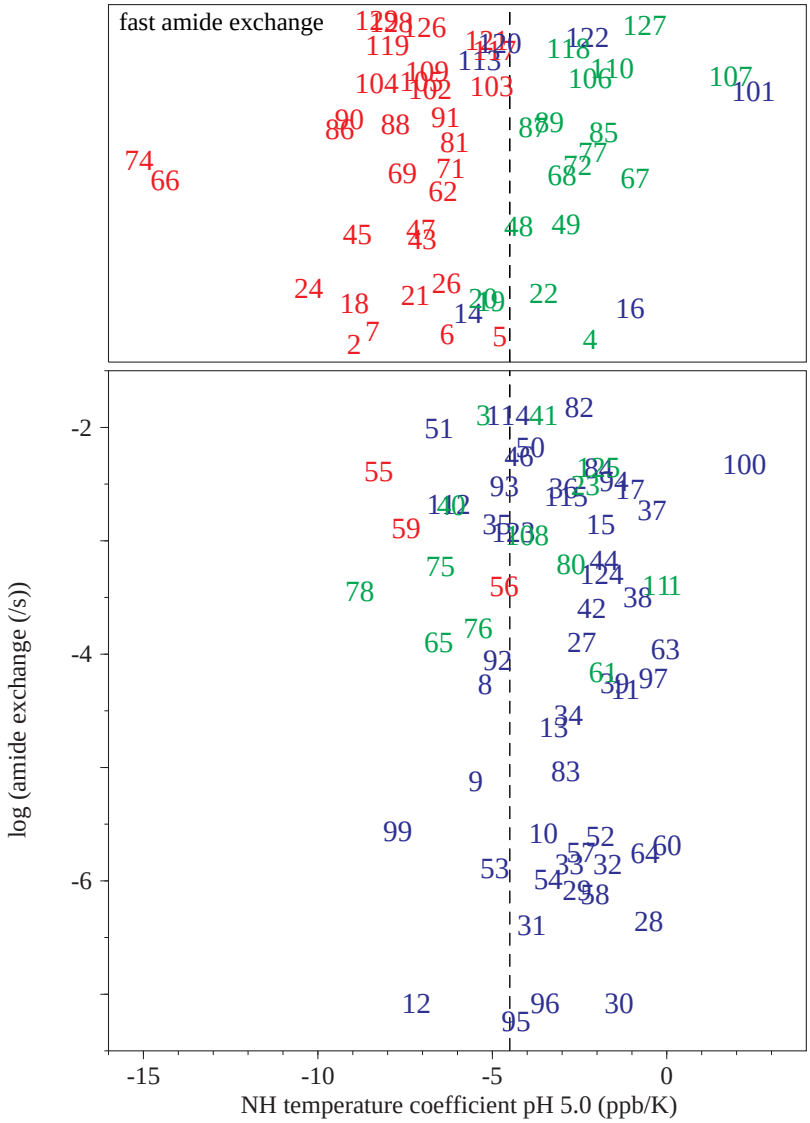

Fig. 5. Correlation between amide proton temperature coefficients for lysozyme at pH 5.0 and the experimentally determined amide exchange rates (Radford et al., 1995). The lower panel illustrates data for which the amide exchange rates were slow enough to be measured. For the amide exchange rates that were too fast to be determined (upper panel), the amide temperature coefficient data are plotted arbitrarily against residue number. Points are marked by residue numbers centered at their respective x and y values and are colored according to red: the absence of a hydrogen bond donor at that residue; blue: the presence of a hydrogen bond donor for that residue present in a well-defined secondary structural motif; green: the presence of a hydrogen bond donor for that residue in a loop region of the protein. The vertical dotted line at a value of –4.5 ppb/K marks the proposed cutoff value for hydrogen-bonded amides.

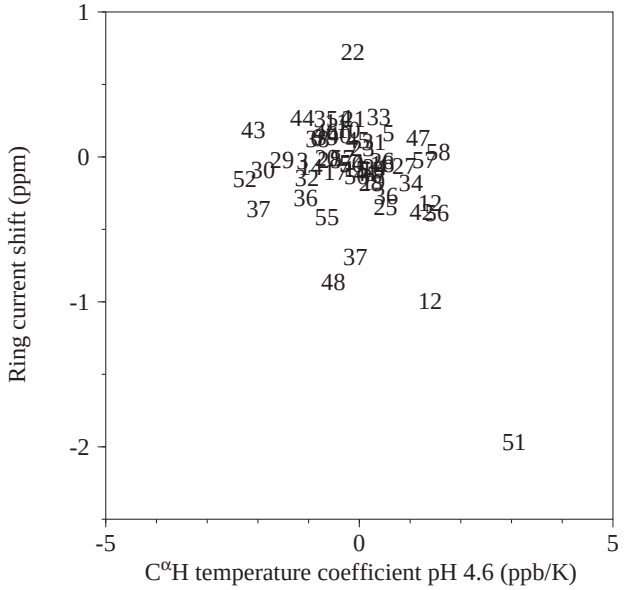

Fig. 6. $C^{\alpha}H$ temperature coefficients for BPTI at pH 4.6 plotted against the calculated ring current shift contribution of the $C^{\alpha}H$ chemical shift. Points are marked by residue numbers centered at their respective x and y values.

are better characterized. It is proposed that if the chemical shift temperature dependences are due to an increase in the local small-scale oscillations of the protein, then the $C^{\alpha}H$ temperature coefficients may be predicted if the local oscillations can be modelled successfully.

As a first attempt, molecular dynamics calculations of BPTI and lysozyme, solvated by explicit water molecules, were used to model the small-scale oscillations. Molecular dynamics trajectories have been reasonably successful in the calculations of dielectric constants (Smith et al., 1993b), structure (Brunne et al., 1995) and order parameters (Smith et al., 1995a), but less so in calculating other dynamic properties (Hünenberger et al., 1995; Smith et al., 1995b). The trajectories are run for a time of the order of nanoseconds, which is too short to reflect slow large-scale motions, but should be long enough to sample the rapid small-scale motions that probably have the most effect on proton chemical shifts. The trajectories for BPTI and lysozyme were generated using GROMOS (van Gunsteren and Berendsen, 1987) at 300 K, using a truncated octahedron box and extended simple point charge (SPC/E) water molecules. For BPTI the last 2.3 ns were taken from a 2.4 ns trajectory, and for lysozyme the last 1 ns was taken from a 1.1 ns trajectory. The trajectories were sampled every 10 ps, yielding instantaneous structures from which chemical shifts were calculated. Average $C^{\alpha}H$ chemical shifts were determined for each residue by averaging the instantaneous shifts over the whole trajectory. In addition, the average protein coordinates were obtained over the trajectory and this was used to calculate the $C^{\alpha}H$ chemical shifts of the average structure. Any difference between the average $C^{\alpha}H$ chemical shifts and the $C^{\alpha}H$ chemical shifts of the average structure is expected to be due to the motion of the protein and should be proportional to the $C^{\alpha}H$ temperature coefficients. Unfortunately there was no correlation between the $C^{\alpha}H$ chemical shift difference and the temperature coefficients (BPTI $C^{\alpha}H$ $R = -0.19$). There are several possible explanations for the disappointing lack of correlation, of which the obvious interpretation is that the trajectories are not accurate enough models of the real motions to yield useful chemical shift calculations.

As a second attempt, we reasoned that if temperature-dependent chemical shift changes are due to an increase in the magnitude of local harmonic oscillations around the mean atomic positions, then they should depend to a first approximation on the calculated difference between the observed $C^{\alpha}H$ chemical shift and the random-coil shift (secondary shift). A reduction in the secondary shift will result from an averaging of the local chemical shift effects due to the thermal oscillations. Such correlations have been seen before for amide protons (Andersen et al., 1992; Rothemund et al., 1996). For $C^{\alpha}H$, no correlation between temperature coefficient and secondary shift was found. However, there was a limited correlation between $C^{\alpha}H$ temperature coefficient and the calculated ring current shift (Fig. 6).

A better approximation of the effect of local oscillations is to calculate the second derivative of the chemical shift with respect to the protein coordinates. When calculated as a torsional oscillation about the C^{γ}-C^{β} axis, no correlation emerged; however, a weak correlation was found when calculated as an isotropic harmonic oscillation of all atoms (Fig. 7). Considering that this calcula-

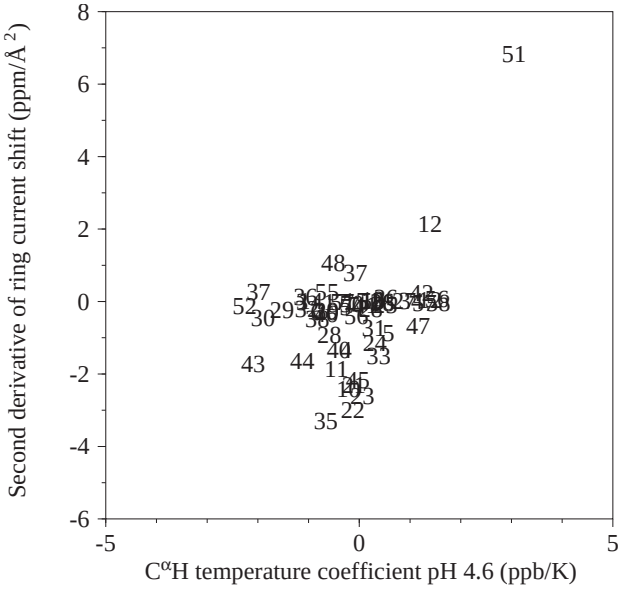

Fig. 7. $C^{\alpha}H$ temperature coefficients for BPTI at pH 4.6 plotted against the calculated second derivative of the ring current shift contribution of the $C^{\alpha}H$ chemical shift. Points are marked by residue numbers centered at their respective x and y values.

tion treats only the ring current shifts and not the other sources of conformation-dependent shift, the level of correlation is reasonable and suggests that our explanation of the origin of the temperature dependence is valid.

Conclusions

Temperature coefficients can be rationalized on the basis of increased thermal fluctuations of the protein at higher temperature, although precise calculations of their magnitudes are poor. They are easily measured, yielding a simple and reproducible parameter which does not display a pH dependence. Amide proton temperature coefficients are reasonably good indicators of hydrogen bonding in globular proteins (whereas in peptides their application is confused by the temperature-dependent loss of secondary structure). Moreover, they are not strongly influenced by surface exposure in contrast to exchange rates, which are strongly correlated to surface exposure. Amide exchange rates and temperature coefficients benefit from being used together as complementary measures of hydrogen bonding. For example, if an amide proton exchanges slowly and has a temperature coefficient more positive than –4.5 ppb/K (bottom right of Fig. 5), it is hydrogen bonded, while if it exchanges rapidly and has a temperature coefficient more negative than –4.5 ppb/K (top left of Fig. 5), it is not hydrogen bonded. Most of the remaining protons are also hydrogen bonded, and, in particular, if a proton has rapid amide exchange but a temperature coefficient more positive than –4.5 ppb/K, it is highly likely to be surface exposed but hydrogen bonded.

Acknowledgements

We thank Dr. A. Mark and Prof. W. van Gunsteren (Zürich) for the molecular dynamics trajectories of BPTI and lysozyme, Dr. J. Craven (Sheffield) for help with the calculations and Dr. N.H. Andersen (Seattle) for sending details of his unpublished work.

References

Andersen, N.H., Chen, C., Marschner, T.M., Krystek Jr., S.R. and Bassolino, D.A. (1992) *Biochemistry*, **31**, 1280–1295.

Asakura, T., Taoka, K., Demura, M. and Williamson, M.P. (1995) *J. Biomol. NMR*, **6**, 227–236.

Bernstein, F.C., Koetzle, T.F., Williams, G.J.B., Meyer Jr., E.F., Brice, M.D., Rodgers, J.R., Kennard, O., Shimanouchi, T. and Tasumi, M. (1977) *J. Mol. Biol.*, **112**, 535–542.

Brunne, R.M., Berndt, K.D., Güntert, P., Wüthrich, K. and van Gunsteren, W.F. (1995) *Proteins*, **23**, 49–62.

Buck, M., Boyd, J., Redfield, C., Mackenzie, D.A., Jeenes, D.J., Archer, D.B. and Dobson, C.M. (1995) *Biochemistry*, **34**, 4041–4055.

Dyson, H.J., Rance, M., Houghten, R.A., Lerner, R.A. and Wright, P.E. (1988) *J. Mol. Biol.*, **201**, 161–200.

Englander, S.W. and Kallenbach, N.R. (1983) *Q. Rev. Biophys.*, **16**, 521–655.

Haigh, C.W. and Mallion, R.B. (1980) *Prog. NMR Spectrosc.*, **13**, 303–344.

Hünenberger, P.H., Mark, A.E. and van Gunsteren, W.F. (1995) *J. Mol. Biol.*, **252**, 492–503.

Hvidt, A. and Nielsen, S.O. (1966) *Adv. Protein Chem.*, **21**, 287–386.

Jiménez, M.A., Nieto, J.L., Rico, M., Santoro, J., Herranz, J. and Bermejo, F.J. (1986) *J. Mol. Struct.*, **143**, 435–438.

Kabsch, W. and Sander, C. (1983) *Biopolymers*, **22**, 2577–2637.

Kurachi, K., Sieker, L.C. and Jensen, L.H. (1976) *J. Mol. Biol.*, **101**, 11–24.

Kurinov, I.V. and Harrison, R.W. (1995) *Acta Crystallogr.*, **D51**, 98–109.

Lee, B. and Richards, F.M. (1971) *J. Mol. Biol.*, **55**, 379–400.

Ohnishi, M. and Urry, D.W. (1969) *Biochem. Biophys. Res. Commun.*, **36**, 194–202.

Ösapay, K. and Case, D.A. (1991) *J. Am. Chem. Soc.*, **113**, 9436–9444.

Pardi, A., Wagner, G. and Wüthrich, K. (1983) *Eur. J. Biochem.*, **137**, 445–454.

Pedersen, T.G., Sigurskjold, B.W., Andersen, K.V., Kjær, M., Poulsen, F.M., Dobson, C.M. and Redfield, C. (1991) *J. Mol. Biol.*, **218**, 413–426.

Pedersen, T.G., Thomsen, N.K., Andersen, K.V., Madsen, J.C. and Poulsen, F.M. (1993) *J. Mol. Biol.*, **230**, 651–660.

Perrin, C.L., Dwyer, T.J., Rebek, J. and Duff, R.J. (1990) *J. Am. Chem. Soc.*, **112**, 3122–3125.

Radford, S.E., Buck, M., Topping, K.D., Dobson, C.M. and Evans, P.A. (1992) *Proteins*, **14**, 237–248.

Redfield, C. and Dobson, C.M. (1988) *Biochemistry*, **27**, 122–136.

Rothemund, S., Weißhoff, H., Beyermann, M., Krause, E., Bienert, M., Mügge, C., Sykes, B.D. and Sönnichsen, F.D. (1996) *J. Biomol. NMR*, **8**, 93–97.

Skalicky, J.J., Selsted, M.E. and Pardi, A. (1994) *Proteins*, **20**, 52–67.

Smith, L.J., Sutcliffe, M.J., Redfield, C. and Dobson, C.M. (1993a) *J. Mol. Biol.*, **229**, 930–944.

Smith, L.J., Mark, A.E., Dobson, C.M. and van Gunsteren, W.F. (1995a) *Biochemistry*, **34**, 10918–10931.

Smith, P.E., Brunne, R.M., Mark, A.E. and van Gunsteren, W.F. (1993b) *J. Phys. Chem.*, **97**, 2009–2014.

Smith, P.E., Van Schaik, R.C., Szyperski, T., Wüthrich, K. and van Gunsteren, W.F. (1995b) *J. Mol. Biol.*, **246**, 356–365.

Thomsen, N.K. and Poulsen, F.M. (1993) *J. Mol. Biol.*, **234**, 234–241.

Tüchsen, E. and Woodward, C. (1987) *Biochemistry*, **26**, 1918–1925.

van Gunsteren, W.F. and Berendsen, H.J.C. (1987) *Groningen Molecular Simulation (GROMOS) Library Manual*, Biomos, Groningen, The Netherlands.

Wagner, G. and Wüthrich, K. (1982) *J. Mol. Biol.*, **160**, 343–361.

Wagner, G., Pardi, A. and Wüthrich, K. (1983) *J. Am. Chem. Soc.*, **105**, 5948–5949.

Wagner, G., Braun, W., Havel, T.F., Schaumann, T., Gō, N. and Wüthrich, K. (1987) *J. Mol. Biol.*, **196**, 611–639.

Waltho, J.P. and Cavanagh, J. (1993) *J. Magn. Reson.*, **A103**, 338–348.

Williamson, M.P., Hall, M.J. and Handa, B.K. (1986) *Eur. J. Biochem.*, **158**, 527–536.

Williamson, M.P. and Asakura, T. (1993) *J. Magn. Reson.*, **B101**, 63–71.

Williamson, M.P., Kikuchi, J. and Asakura, T. (1995) *J. Mol. Biol.*, **247**, 541–546.

Wlodawer, A., Walter, J., Huber, R. and Sjolin, L. (1984) *J. Mol. Biol.*, **180**, 301–329.

Woodward, C., Simon, I. and Tüchsen, E. (1982) *Mol. Cell. Biochem.*, **48**, 135–160.

Wüthrich, K. (1986) *NMR of Proteins and Nucleic Acids*, Wiley, New York, NY, U.S.A.